Design and characteristic research on side-polished fiber fluid sensing system*

LIU Yu (刘宇), **YANG Qingrong** (杨庆荣), **LU Yongle** (路永乐), **DI Ke** (邸克), **WEN Dandan** (文丹丹), **YUE Yiting** (岳怡婷), **ZHOU Min** (周敏), **WANG Changle** (王昌乐), **and GUO Junqi** (郭俊启)**

Chongqing Engineering Research Center of Intelligent Sensing Technology and Microsystem, Chongqing University of Posts and Telecommunications, Chongqing 400065, China

(Received 14 November 2020; Revised 17 December 2020)

A novel fluid sensing system based on side-polished optical fiber (SPOF) is proposed, which realizes the fluid replaceability and effective refractive index (RI) sensing characteristics. Numerical investigations demonstrate that the photonic bandgap effect can be obtained if the RI of liquid is higher than that of substrate material in the wavelength range studied. The relationship between bandgap edge wavelength and RI is studied theoretically. The SPOF with a depth of 57 μm is used in the experiment to realize the construction of the fluid channel. After filling three different liquids, the result shows that the wavelength of the bandgap edge has a red shift with RI increased, which is nearly linear in the RI range of 1.56—1.6 with a sensitivity about 5 543.64 nm/RIU. The proposed sensing system can be flexibly applied to the field of fluid characteristic sensing such as biochemical solution characteristic detections.

Document code: A **Article ID:** 1673-1905(2021)08-0490-6

DOI https://doi.org/10.1007/s11801-021-0182-7

Photonic crystal fibers (PCFs) with regular air holes are easy to be combined with functional materials to design optical fiber sensors with high sensitivity[1,2]. At present, the performance of material filling technology is limited in mixed liquid detection and repeatable operation because it is difficult for the materials to be replaced, updated and mixed during the process of optical fiber sensing when the material needs to be filled into the internal fiber in advance[3-9]. The development of fluid sensing system breaks through this limitation and the real-time monitoring of internal fluid materials is achieved through the detection of optical signals[10-14]. Therefore, it is great significance for academic to study the fluid control technology with stable structure, flexible design, and high integration.

To achieve the goal of repeatedly replacing the filling fluid inside the PCF and real-time monitoring of sensor data, X. Yang et al[15] realized a channel of microfluid by etching microholes for inlets and outlets on the surface of the optical fiber. The linear sensing range of 0.1—4.0 mmol/L of H_2O_2 concentration is obtained by the systems. while the micromachining technique requires high-accuracy positioning stages, making it difficult to popularize. C. Wu et al[16] from Korea demonstrated a highly sensitive microfluidic refractometer based on an SMF-C-PCF-C-SMF structure, while the tiny C-shaped fiber brings difficulty in manipulation and the light leaked seriously for transmitting in liquid core. N. Zhang et al[17] used a sloped fiber to achieve fluid control in a side-channel PCF. However, the opening is not large enough through the fusion splicing with inclination angle, which limits the flow rate and reduces stability. In 2018, Chen X et al[18] designed a D-shaped PCF with a laterally accessible hollow-core. A side-opening channel is introduced to allow the analyte to gain access to the fluid channel, which also provides a possibility for real times sensing. However, the fluid channel is far away from the core, which limits the detection sensitivity. In summary, the current optical fiber fluid control technology has achieved certain research results, but they cannot meet the requirements of replaceable filling liquid through simple processing technology, which limits the application scope of this technology.

Based on the deficiency mentioned above, we propose a neotype fluidic sensing system based on side-polished optical fiber (SPOF). The outstanding advantage of this solution is that the goals of repeated replacement and mixing of the target fluid solution are achieved, and the air hole location of the fluidic channel can be flexible control by adjusting. Various filling schemes can be de-

* This work has been supported by the National Key Research and Development Program of China (Nos.2018YFF01010202 and 2018YFF01010201), the National Natural Science Foundation of China (Nos.61705027 and 11704053), the Innovation Leader Talent Project of Chongqing Science and Technology (No.CSTC-CXLJRC201711), the Basic Research Project of Chongqing Science and Technology Commission (No.CSTC-2018jcyjax0619), and the Science and Technology Research Project of Chongqing Education Commission (No.KJQN201900615).

** E-mail: guojq@cqupt.edu.cn

signed for the fluidic system proposed in this paper, and it is of great significance to realize effective schemes through experimental research. In this paper, three liquids with high refractive index (RI) are injected into the fluid sensing system, the result shows that the wavelength of the band gap edge has a red shift with RI increased. it is preliminarily determined that it has fluid replaceability and RI sensing properties based on the photonic bandgap theory. To obtain accurate relative sensitivity, the RI of the solution is controlled by a high-precision temperature control box. Results of sensing experiments show that the edge wavelength of the bandgap exhibits a highly sensitive response to the RI of the fluid. For the temperature-sensitive filling liquid filled in this article, the RI sensitivity of the microfluidic device is 5 543.64 nm/RIU.

As shown in Fig.1, the experimental setup includes a supercontinuum light source, a section that filling fiber into the temperature chamber, and an optical spectrum analyzer (OSA). The spectrum range of the light source ranges from 600 nm to 1 700 nm, the highest resolution of the OSA is 0.02 nm, and the resolution we used in the experiment is 0.1 nm.

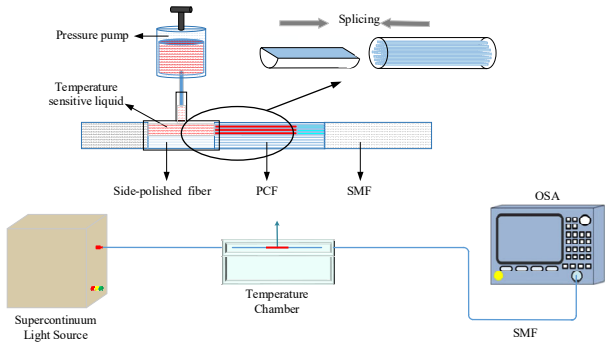

Fig.1 Schematic diagram of the experimental setup for the measurement

A neotype fluidic sensing system based on SPOF is shown in the inset of Fig.1. The cross-section of the PCF is shown in Fig.2(a), which is manufactured by Yangtze Optical Fiber and Cable Company Ltd. of China. The filling length is about 6 cm. The cross-section of the SPOF is shown in Fig.2(b), and the cross-section of the filled PCF is shown in Fig.2(c). The RI of the filled liquid in this experiment is higher than that of PCF silica, which results in a photonic bandgap effect after the liquid is injected into the PCF. When we spliced the fiber with standard single mode fiber, the air holes of ends of the PCF were left without fluid for the reduction of the splice loss.

The parameters that affect the optical performance of the SPOF mainly include the precise polishing depth and length of the fiber, power loss as well as the surface quality of the fiber. The preparation method used in this experiment is a wheeled mechanical polishing method that has the advantages which are simple production process, safety and flexibility and adjustable polishing depth and length. The processing steps are mainly divided into four steps: Rough grinding, fine grinding, fine polishing, and fire polishing. After the previous processing steps, an SPOF with fewer surface scratches can be obtained. Because high temperature discharge can further improve the smoothness of the polished surface, so the SPOF can be prepared with good surface quality After all the steps have been completed, the preparation of the SPOF can be completed. Fig.3(a) shows the physical image of the processed SPOF under a magnifying glass. The specific processing dimensions are the polishing depth of 57 μm and the polishing length of 2 cm. This depth is just enough to make the liquid integrate into the air hole with a depth of 5 layers. The closer the high RI liquid is to the core of fiber, the more likely it is to produce the photonic bandgap phenomenon.

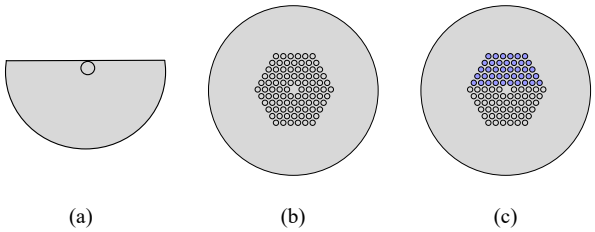

Fig.2 Cross-sections of (a) the SPF, (b) the PCF and (c) the filled PCF

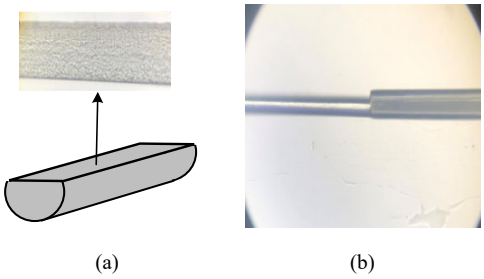

Fig.3 (a) Physical image of the processed SPOF under the microscope; (b) Physical picture of SPOF-PCF after splicing

The fusion splicing process of the SPOF and the microstructure fiber of the fluid control system is mainly divided into two parts: Alignment of the fiber end face and optimization of the splicing parameters. The manual splicing mode of the polarization maintaining splicer can be used to align the end faces of the SPOF and the micro-structured optical fiber. The next step is to optimize the welding parameters by adjusting the two parameters of discharge intensity and discharge time. Compared with the fusion parameters of SMP-PCF (the discharge intensities are 40 bit and 60 bit, and the discharge time is 1 000 ms), in order to prevent the collapse of cladding air hole caused by excessive discharge intensity, the discharge intensity

should be appropriately reduced in the fusion process of SPOF and PCF.

The fusion machine adjusts the parameters in real time according to the welding situation. After several comparisons to ensure the fusion quality, 25 bit of discharge intensity and 1 000 ms of discharge time were finally selected as the welding parameters. When the splicing of the SPOF and the PCF are completed, the other end of the PCF and the ordinary single-mode fiber are spliced to complete the construction of the single-sided fluid control system. The physical map after splicing is shown in Fig.3(b). It can be confirmed that, by observing the output spectrum, the optical path of the optical fiber fluid control system designed in this paper is successfully constructed, and the optical signal can be detected by the spectrometer (OSA).

The band gap fiber made in this paper uses fluid control technology to inject liquid into a solid-core PCF, causing the cladding RI to be higher than that of the core, and the light guiding mechanism is changed from RI guided to photonic band gap. When the wavelength is at the band gap boundary, the high RI liquid column generates a conductive mode, which makes the core part of the energy coupled into the cladding, and light cannot be confined to transmit in the core at this time. When the wavelength is in the center of the band gap, the core mode and the cladding mode hardly resonantly couple, and the light is restricted to be conducted in the core. The position and width of the photonic band gap also change When the RI of the liquid changes. In order to perform numerical calculations on the filled fiber, this experiment uses the photonic crystal band structure calculation software MPB (MIT Photonic Bands). The plane wave expansion method is used to theoretically calculate the bandgap change. Due to the limitation of the drawing process, neither the air hole diameter nor the hole spacing is completely consistent with the actual parameters. This will not have much impact on theoretical analysis. The model established in MPB is an ideal fiber structure model.

The filled liquid is a temperature-sensitive liquid made by the Cargille laboratory. Its RI is measured at a temperature of 25 °C and a wavelength of 589.3 nm. In the simulation, the material dispersion should be properly considered. The RI of the core material at 1 500 nm is 1.444. There is an effective core conduction mode inside the bandgap where the effective RI of the mode is less than 1.444. After filling the pores of the optical fiber cladding with high RI matching liquid, the optical fiber becomes a photonic bandgap optical fiber. The simulation result of the bandgap of the filled liquid with an RI of 1.6 is shown in Fig.4. A photonic bandgap centered at 1 200 nm appears in the wavelength range of 1 100 nm to 1 300 nm.

Repeat the above experiment, fill two high RI liquids with RIs of 1.58 and 1.56, respectively, and analyze the RI response characteristics of the bandgap. The change of the bandgap RI sensitivity with wavelength is shown in Fig.5. When the RI of the liquid is 1.58, the wavelength range of the bandgap is from 1 050 nm to 1 200 nm, and the center wavelength is about 1 100 nm. When the RI of the liquid is 1.56, the wavelength range of the bandgap is from 950 nm to 1 125 nm, and the wavelength of the center of the bandgap is at 1 080 nm. So far, by filling the high RI liquid into the cladding air hole of the PCF, the conduction mechanism is changed. The RI guiding mechanism becomes the photonic bandgap guiding mechanism. There is a wide transmission window in the wavelength range of 1 000—1 300 nm, which provides convenience for subsequent research on the mechanism and application of bandgap reduction.

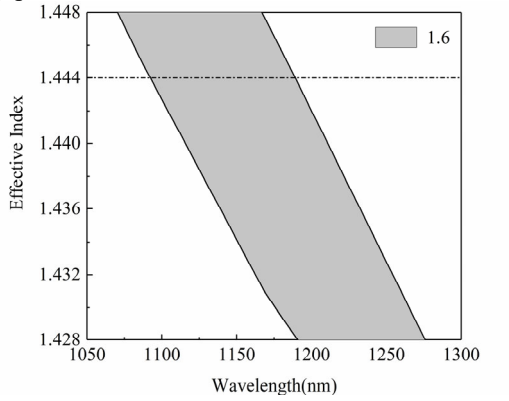

Fig.4 Bandgap diagram of fiber filled with a liquid with RI of 1.6

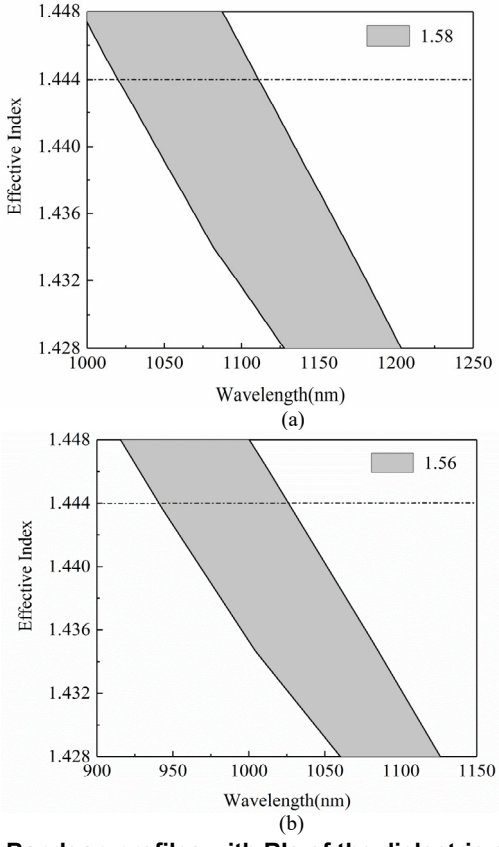

Fig.5 Bandgap profiles with RIs of the dielectric columns of (a) 1.58 and (b) 1.56

Fig.6 shows the distribution of the long-wave boundary of three different RIs (1.6, 1.58 and 1.56) in the wavelength range of 1 000—1 300 nm. As the RI increases, the band gap drifts toward the longwave direction, and the drift speed of the longwave boundary is about 5 000 nm/RIU. Due to the dispersion effect, the wavelength change will cause the RI of the fluid material to change, so that the bandgap is not translated as a whole during the drift process, and the width will change accordingly.

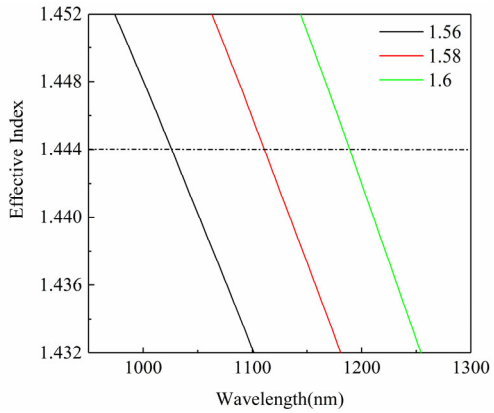

Fig.6 Theoretical calculation of bandgap distribution at different RIs

Based on the above theory, specific experimental verification is carried out. Firstly, the liquid with RI of 1.6 is introduced into the fluid channel by a pressure device. The transmission spectrum of this system at room temperature is shown in Fig.7(a), and it can be observed that there is an obvious photonic bandgap phenomenon. After that, the system is filled with high-RI liquids with RIs of 1.58 and 1.56, respectively. It can be seen from Fig.7(b) that the whole bandgap moves towards the direction of long wave with the increase of RI. At the same time, the bandgap edge in the long wave range moves faster than that in the short wave range. This means that the bandgap is not only red shifted, but each bandgap is compressed as the RI decreases.

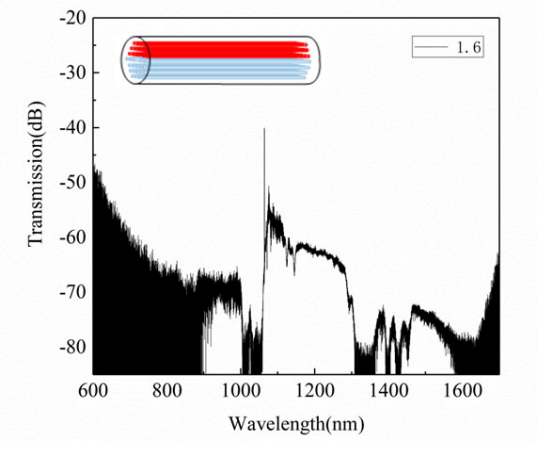

(a)

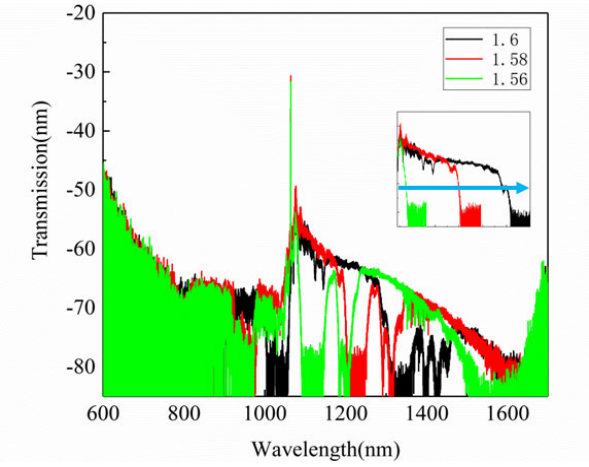

(b)

Fig.7 (a) Transmission spectrum of the filled liquid with the RI of 1.56; (b) Transmission filled with liquid with different RIs

In order to further study the sensing characteristics of the RI of the fluid system, the fluid material with a small RI range can be filled. The drift characteristics of the fixed point with the change of RI can be observed in the transmission spectrum, and the functional relationship between the wavelength position of the observation point and the RI can be established. Usually, it is not accurate enough for the method to configure a large number of liquids with different RIs in a small range by using an Abbe refractometer; therefore, the method selected in this experiment is to fill the fluid control system with temperature-sensitive liquid. Then the RI of the temperature-sensitive liquid which is calculated according to the thermo-optical coefficient, adjusted accurately through a high-precision temperature control box. Finally, the RI can be sensed through the analysis of the change of the corresponding wavelength in the real-time transmission spectrum.

Firstly, the temperature-sensitive liquid produced by Cargille Laboratories Inc is filled, which a temperature of 25 °C, has an RI of 1.58 at a wavelength of 589.3 nm, and has a thermal optical coefficient of −0.000 404 $°C^{-1}$. The temperature was set to 25 °C and the transmission spectrum of the PCF was measured, and the spectrum was smoothed with a filter. Multiple distinct bandgaps were observed at the wavelength of 600—1 700 nm. Then a temperature control box was used to increase the temperature from 25 °C to 75 °C with a temperature interval of 5 °C. According to the thermo-optical coefficient of the heat-sensitive liquid, it can be calculated that the RI varies from 1.58 to 1.559 8 with an interval of −0.002 2. And then we got the drift curve of the transmission spectrum with the RI of 1.58 as shown in Fig.8(a). It can be found that the RI of liquid becomes smaller and the edge of the band gap moves to the shortwave direction as the temperature rises.

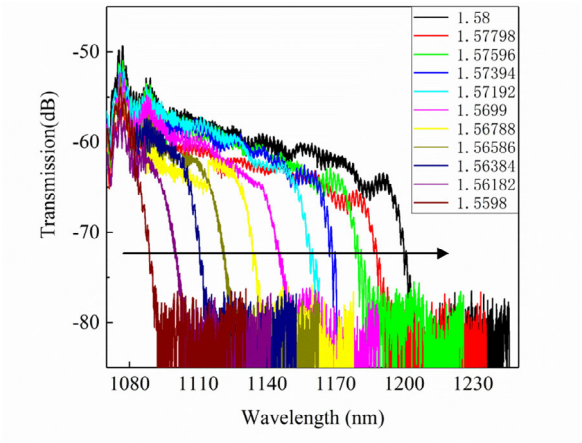

(a)

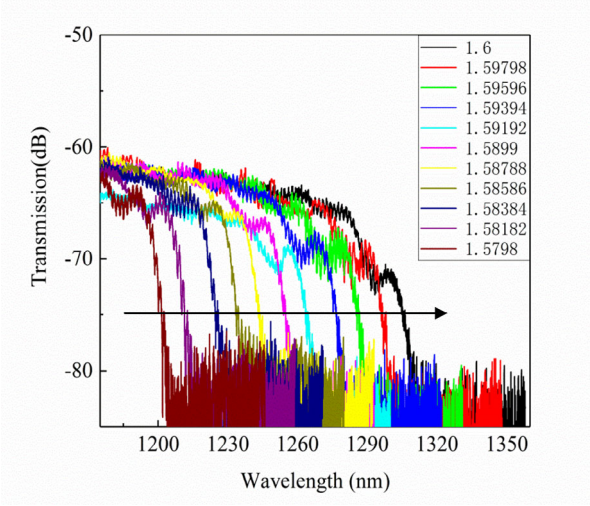

(b)

Fig.8 Bandgap edge drift characteristics of photonic bandgap fibers filled with liquids with RIs of (a) 1.58 and (b) 1.6

To verify the universality of the sensing system, the temperature-sensitive liquid with RI of 1.58 in the fluid system is completely removed by using a vacuum pump. The functional material in the fluid channel is replaced with a temperature-sensitive liquid with the RI of 1.60, and the vacuum pump is used again to push the liquid into the air hole channel of the fluid system to complete the replacement of the liquid. Then a temperature control box is used to increase the temperature from 25 °C to 70 °C with a temperature interval of 5 °C. According to the thermo-optical coefficient of the heat-sensitive liquid, it can be calculated that the RI varies from 1.60 to 1.581 82 with an interval of −0.002 02. The drift curve of the transmission spectrum with RI of 1.6 is shown in Fig.8(b).

In order to further analyze the RI response characteristics of the bandgap, two sets of experimental data with filled RIs of 1.58 and 1.6 were integrated. The right edge of the bandgap with a fixed loss of −74 dB is selected as the observation object. It is found that the drift characteristic of the bandgap edge with the change of RI is approximates linear, the linear fitting is performed as shown in Fig.9. A linear fitting degree of 99.96% is obtained, and the slope of the linear fitting can be used to express the RI sensitivity. The calculated RI is in the range of 1.56—1.6, and the RI sensing sensitivity of the system is 5 543.64 nm/RIU. The theory accords well with the experiment.

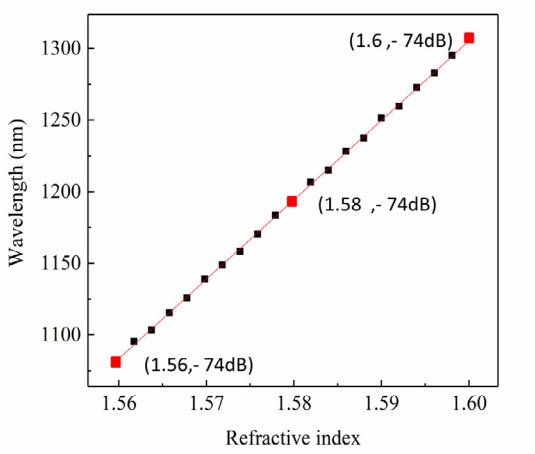

Fig.9 Fitting curve of RI and left edge wavelength of bandgap

In conclusion, we have demonstrated a novel sensing system based on SPOF, which can produce the obvious photonic bandgap effect. The RI sensing characteristics of the fluid control system is studied by analyzing the change of the edge of the photonic bandgap, and the response results with good linearity are obtained. In the range from 1.56 to 1.6 of RI, the high sensitivity is up to 5 543.64 nm/RIU, which is consistent with the drift direction and drift velocity of the bandgap in the wavelength range of 1 000—1 300 nm simulated by MPB. Some of the difference is caused by the deviation between the optical fiber parameters in the theoretical model and the actual optical fiber parameters. But these differences don't affect the results of the experiment. Because of the advantages which are the structure with high sensitivity, easy manufacturing, compact structure and low loss, this system can be applied to the RI of other fluid materials, concentration, temperature and other related physical characteristics detection.

References

[1] Morshed M, Imran Hassan M, Roy Tusher Kanti, Uddin Muhammad Shahin and Abdur Razzak S M, Appl. Opt. **54**, 8637 (2015).

[2] Ertman S, Lesiak P and Tomasz R Woliński, Journal of Lightwave Technology **35**, 3399 (2017).

[3] Wang D, Chen G and Wang L, Optical Fiber Technology **29**, 95 (2016).

[4] Sławomir Ertman, Piotr Lesiak and Tomasz R Woliński. Journal of Lightwave Technology **35**, 3399 (2017).

[5] Qiang Liu, Liang Xing and Zhaoxia Wu, Optics Communications **452**, 238 (2019).
[6] Xiang Zi Ding, Hang-Zhou Yang, Xue-Guang Qiao, Pan Zhang, Oin Tian, Qiang Zhou Rong, Nurul Asha Mohd Nazal, Kok-Sing Lim and Harith Ahmad, Applied Optics **57**, 2050 (2018).
[7] Reyes Vera Erick, Cordeiro C M B and Pedro T, Applied Optics **56**, 156 (2017).
[8] Bai J, Ge M, Wang S, Yang Y, Li Y and Chang S, Optics Communications **419**, 8 (2018).
[9] Geng Y, Xu Y, Tan X, Wang L, Li X, Du Y and Hong X, Sensors **18**, 1726 (2018).
[10] Zhao L, Han H, Lian Y, Luan N and Liu J, Optical Fiber Technology **50**, 165 (2019).
[11] Boufenar R, Bouamar M and Hocini A, Advanced Electromagnetics **7**, 11 (2018).
[12] Rifat A A, Mahdiraji G A, Sua Y M, Shee Y G, Ahmed R and Chow D M, IEEE Photonics Technology Letters **27**, 1628 (2015).
[13] Hou M, Wang Y, Liu S, Li Z and Lu P, IEEE Sensors Journal **16**, 6192 (2016).
[14] Huang Y, Wang Y, Zhang L, Shao Y, Liao C and Wang Y, Journal of Lightwave Technology **37**, 1903 (2019).
[15] Yang X, Yuan T, Yang J, Dong B, Liu Y, Dong B, Liu Y, Zheng Y and Yuan L, Optics Letters **38**, 3433 (2013).
[16] Kassani S H, Park J, Jung Y, Kobelke J and Oh K, Optics Express **21**, 14074 (2013).
[17] Iokibe K, Tai N, Kagotani H, Onishi H and Watanabe T, IEEJ Transactions on Fundamentals and Materials **136**, 365 (2016).
[18] Chen X, Xia L and Li C, IEEE Photonics Journal **10**, 1 (2018).